THE JOURNAL OF PHYSICAL CHEMISTRY B LETTERS

2005, *109,* 20051−20054
Published on Web 10/07/2005

Modeling of Crystallization Process in Confined Melt of Sulfuric Acid Catalyst

Dmitrii Efremov,* Vladimir Elokhin, and Bair Bal'zhinimaev

Boreskov Institute of Catalysis, pr. Lavrentieva, 5, 630090 Novosibirsk, Russia

Received: May 20, 2005; In Final Form: September 21, 2005

Metropolis Monte Carlo technique has been applied to simulate the crystallization process in the melt of vanadium sulfuric acid supported catalysts. The melt is a lattice binary compound consisting of $(V^{4+})_2$ and $(V^{5+})_2$ binuclear complexes (dimers) confined by pore walls of cylindrical or slitlike shape. It has been shown that the crystallization process retards significantly as the pore size decreases. This result is in good agreement with the experimental data obtained earlier. The effect of the energy properties of pore walls (attractive, repulsive, or inert) on the crystallization features has been studied as well.

Introduction

It is well-known that at low temperatures the active V(V) binuclear complexes in the melt of the active component of vanadium catalyst for SO_2 oxidation are partly reduced to V(IV) ones which are crystallized to solid V(IV) compound.[1−3] This phenomenon results in sharp drop of catalytic activity.[1,2] The crystallization (deactivation) process is strongly affected by the chemical composition of the active component (Me/V ratio, Me = Cs, K, Na) as well as by the features of the support (SiO_2) porous structure.[4] It was found experimentally that the smaller the support pore size, the higher the catalytic activity due to significant retarding of the crystallization process.[4] The activity of the catalyst with a mean pore size of 10 nm was 5−10 times higher than that for samples with pore sizes of 50−200 nm in the same low temperature region (620−670 K).[4]

The present letter is devoted to modeling of the crystallization process in pores with different sizes, and the main idea of our simulation studies is a correspondence between the precrystallization state determined by the self-organized set of dimers and the average potential energy of the melt, from one side, and the diameter of pore, from another one.

Description of Lattice Melt Confined by Pore Walls

The statistical lattice model for the binary V(V)−V(IV) homogeneous melt was described in detail earlier.[5−7] The melt of active component is considered as a cubic lattice of N cells with periodic boundary conditions. Each cell contains one of the binuclear complexes, $(V^{4+})_2$ or $(V^{5+})_2$. Note that each complex comprises two vanadium atoms surrounded by some ligands, which are not of importance for the model considered. There are only four reciprocal orientations of two neighboring dimers: (1) consecutive (- -), (2) parallel (||), (3) perpendicular ($\perp$), and (4) crossed ($\times$). It was assumed for simplicity that the pairwise interaction energies dealt with the neighboring perpendicular and crossed orientations are zero whereas nonzero interaction between dimers supposed to occur for either consecutive or parallel configurations. This means that there are only six different (attractive) pairwise interaction energies between the neighboring complexes of $(V^{4+})_2 \leftrightarrow (V^{4+})_2$, $(V^{4+})_2 \leftrightarrow (V^{5+})_2$, and $(V^{5+})_2 \leftrightarrow (V^{5+})_2$ dimers denoted below as E_{44}^{--}, $E_{44}^{||}$, E_{45}^{--}, $E_{45}^{||}$, E_{55}^{--}, and $E_{55}^{||}$. At a certain temperature, the dimer concentration ratio $(V^{4+})_2/(V^{5+})_2$ is constant and it can be calculated from the reaction kinetics[3,8] at a given temperature and the gas composition (i.e., O_2, SO_2, and SO_3 partial pressures). The dimer concentration ratio at a given temperature is a key parameter for the initial seeding procedure which consists of random choices of orientations and space positions for all of the N dimers. As we have dealt with the simulations at constant temperature, volume, and a number of dimers, any lattice melt configuration, ξ, should be considered as an element of canonical statistical ensemble and, therefore, the Metropolis method[9,10] can be applied to study this model melt, as described below.

As for the confined melts, it was assumed additionally in the present work that the model binary compound was bounded by the walls of cylindrical or slitlike pores of different sizes measured here by the number of lattice positions per diameter of cylinder or per slitlike pore width. In the case of cylinders, one of the Cartesian axes (for instance, *k*) was considered as an axis of the cylindrical pore belonging to the more extended lattice. The point of origin of such a coordinate system was placed in the middle of a *k*-axis, and all of the lattice nodes with integer coordinates *i* and *j* satisfying to inequality

$$i^2 + j^2 \le (\text{pore·radius})^2 \qquad (i, j, k = 0, \pm1, \pm2, ...) \quad (1)$$

were exposed to the initial random seeding with $(V^{IV})_2$ and $(V^{V})_2$ complexes (see the next section). The other lattice nodes, that is, possessing *i* and *j* coordinates such as

$$i^2 + j^2 > (\text{pore·radius})^2 \qquad (i, j, k = 0, \pm1, \pm2, ...) \quad (2)$$

were considered as atomic units of a model support; however, only the nearest to the cylindrical surface exterior could interact with neighboring melt dimers in some cases. These pairwise solid/melt interactions were supposed to be attractive, repulsive, or zero.

10.1021/jp052642k CCC: $30.25

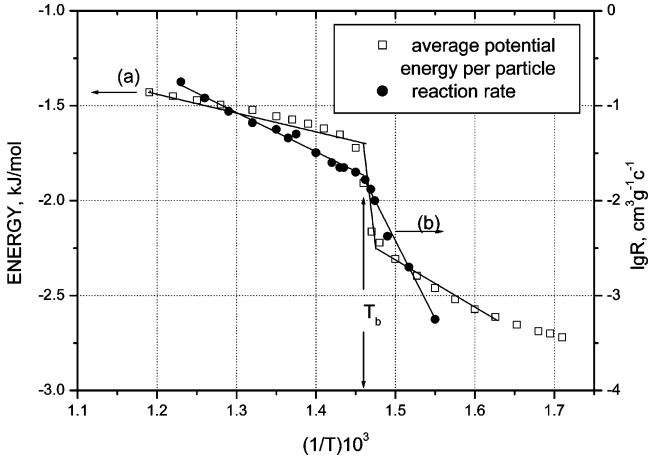

Figure 1. Temperature dependencies of SO_2 oxidation reaction rate (black circles) and equilibrium potential energies per cell (open squares) calculated by canonical Monte Carlo for the case of the bulk melt.

The case of slitlike pores from a simulation point of view is distinguished from the case of cylindrical pores only by the coordinate limitations, that is,

$$|k| \leq 0.5H \qquad (k = 0, \pm1, \pm2, ...) \tag{3}$$

for the melt cells (H is the pore width) and

$$|k| > 0.5H \qquad (k = 0, \pm1, \pm2, ...) \tag{4}$$

for the support ones.

Simulation Algorithm

It is clear from the above section that the simulation study of a melt confined by pore walls needs appropriate values of the pairwise energies E_{44}^{--}, $E_{44}^{||}$, E_{45}^{--}, $E_{45}^{||}$, E_{55}^{--}, and $E_{55}^{||}$. In earlier studies,[5−7] these energy values have been determined on the basis of the hypothesis that the catalyst activity reduction correlated strongly with the crystallization of V(IV) species and, as a consequence, with the lowering of the total melt potential energy. In particular, such a conception assumes that the Arrenius plot breakpoint, T_b, coincides with the temperature breakpoint of the e_ξ versus $10^3/T$ curve, where the symbol e_ξ means the equilibrium average potential energy of simulated dimer configurations per cell. Figure 1 presents an example of experimental SO_2 oxidation rates and corresponding calculated average potential energies per cell versus $10^3/T$ for the K/V catalyst with a pore diameter of ∼100 nm at 85% SO_2 conversion.[2] In this case, the average potential energy per cell versus $10^3/T$ has been calculated for an "infinite" lattice (with periodic boundary conditions). In the following, this lattice is referred to as the "bulk" melt. Absolute V^{4+} concentrations were obtained at every T from a kinetic model.[3,8] The best agreement between breakpoint positions on these two curves was found at the following pairwise interaction energy values: $E_{44}^{--} = -3.78$ kJ/mol, $E_{45}^{--} = -3.63$ kJ/mol, $E_{55}^{--} = -3.16$ kJ/mol, $E_{44}^{||} = -2.95$ kJ/mol, $E_{45}^{||} = -3.2$ kJ/mol, and $E_{55}^{||} = -2.55$ kJ/mol. Note that these energy values differ slightly from the previous ones.[5] These differences were provided by more careful and long-time fitting calculations carried out in the frame of the present study. Energy values, E_{ij}, of that order of magnitude reflect weak dipole/dipole or ion/dipole interaction, and they are most likely necessary to maintain the optimal configuration for the phase transition. The obtained pairwise energies of interaction between dimers together with three types of energies of interaction between vanadium complexes and pore wall cells

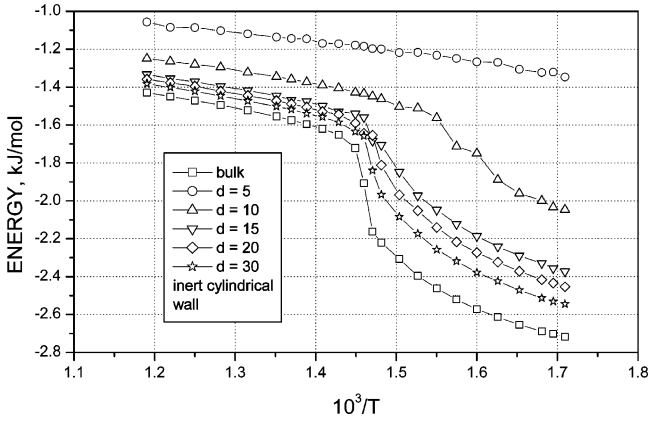

Figure 2. Calculated equilibrium potential energies per cell of melts confined by cylindrical walls of different diameters, d, vs inverse temperature: circles, $d = 5$; up triangles, $d = 10$; down triangles, $d = 15$; diamonds, $d = 20$; stars, $d = 30$; squares, $d =$ infinity (bulk melt).

($E_w = 0$, $E_w = +1$, and $E_w = -1$ kJ/mol) were used in the Monte Carlo (MC) simulations of the melt confined by cylindrical and slitlike pore walls. Note that the chosen nonzero values of E_w correspond to ∼ −120 K (120 K) in terms of well depth divided by Boltzman constant. It is 2−3 times greater than well-known values of the solid/fluid potential well depths in the case of silica and simple Lennard-Jones fluids. Therefore, it seems that the value 1 kcal/mol chosen here is quite reasonable. The initial coordinates and orientations of dimers in any case were chosen using a random number generator taking into account inequalities 1 and 2 established for cylinders or conditions 3 and 4 for the slitlike pores. In the case of cylindrical pores, the periodical boundary conditions were imposed along the cylinder axis, k, while, in the case of slitlike pores, these conditions took place in the lateral directions (i and j). To equilibrate the system, $0.5N \times 10^3$ configurations were generated. Then, the next $5.0N \times 10^3$ configurations were used for averaging. Note that we used "double" MC trials in our MC simulations: any trial consisted of attempts to transform the randomly chosen dimer into another state (1) by changing its space orientation and (if this changing was successful) (2) by the subsequent attempt to change a space position with another randomly chosen dimer. The success of each of these two attempts was checked by the inequality

$$\chi > \exp\{[E_i(\xi) - E_f(\xi)]/RT\} \tag{5}$$

Here, E_i and E_f are the potential energies of the system before and after the MC trial, respectively; T is the temperature; $R = 0.008\,31$ kJ K^{-1} mol^{-1} is the gas constant; and χ is the pseudorandom number from the interval (0,1). Note that the probability criterion 5 supposes that the pairwise energies are expressed in units of kilojoules per mole.

Results and Discussion

Figure 2 presents the melt equilibrium potential energy per cell versus $10^3/T$ for the several diameters, d, of the cylindrical pores and for the bulk melt (the lowest curve). It is clear that reduction in the pore diameter leads to noticeable changes in the energy curve behavior in the low temperature region. The sharp drops of the energies in the vicinity of T_b become smoother with decreasing pore size. Moreover, the smaller the pore diameters, the more shifted the temperature breakpoint, T_b, toward the lower temperatures, especially for the pore diameters of 5−15 dimers in size. According to the above base conception concerning the correlation between reaction rate, crystallization

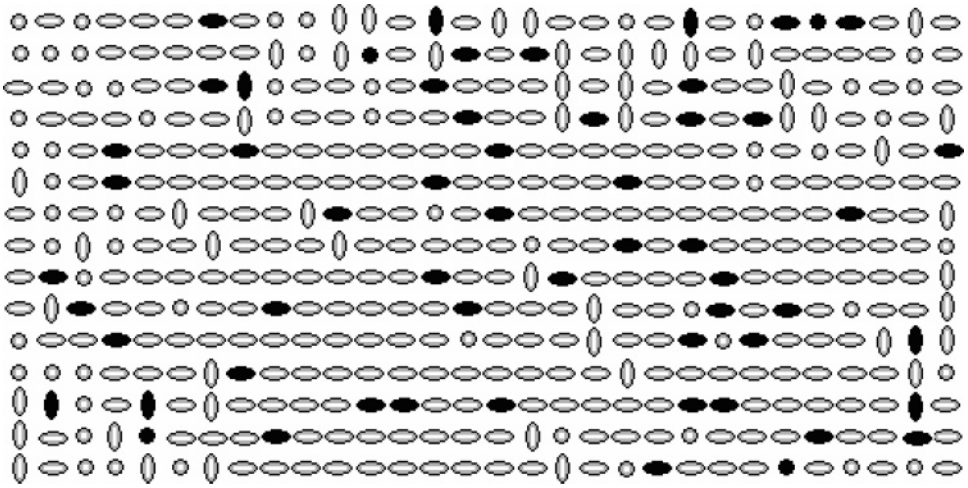

Figure 3. Snapshot of the axial cylinder section ($d = 15$ dimers) for the final momentary configuration of the dimeric compound (Figure 2, $10^3/T = 1.5$): the dark figures are $(V^{5+})_2$ complexes; the bright figures correspond to $(V^{4+})_2$ dimers.

level, and average potential energy (see the beginning of the previous section), one can conclude that the pore size reduction hampers the melt crystallization and, as a consequence, inhibits the sharp reduction of the SO_2 oxidation rate.

Further, on the basis of the behavior of the energy curves in the low temperature region, one may presuppose that the pore diameters of 5−15 dimers in length are the most favorable for SO_2 oxidation because of the relatively high values of the average potential energy and, as a consequence, lower levels of crystallization. Taking into account the linear sizes of vanadium complexes (together with its ligand envelops) of ∼1.0 nm,[11] it may be concluded that the pore diameters of ∼15 nm and smaller provide high catalyst performance in SO_2 oxidation at low temperatures. This observation is in good agreement with the earlier experimental results: the catalytic activity on the support with a pore size of ∼10 nm was 5 times higher at 620−670 K than in the case of supports with pore sizes of 50−100 nm.[4]

Figure 3 presents the final momentary configuration of dimers (snapshot) in the (*j*,*k*) central section of the cylindrical pore of 15 dimers in diameter at $10^3/T = 1.5$ (i.e., 667 K). The bright particles are the $(V^{4+})_2$ complexes, while the dark ones are the $(V^{5+})_2$ dimers. The particles oriented along the *j* and *k* directions have an ellipsoidal shape, whereas the circles indicate the orientation of dimers which is perpendicular to the (*j*,*k*) plane. It is clear from Figure 3 that most of the dimeric axes are oriented along the cylinder axis (*k* direction). Such a behavior differs essentially from the crystallization pictures of the bulk melt (see, for instance, Figure 1b in ref 7). Indeed, in the bulk melt, the clustering of dimers occurs toward all three possible coordinate directions, while the cylindrical wall affects the crystallization character in such a way that only one axial direction is preferable. The latter observation was justified for all three types of dimer/support interactions (i.e., for the attractive, repulsive, and inert walls).

Figure 4 presents the melt equilibrium potential energy per cell versus $10^3/T$, for the different widths, *H*, of slitlike pores and for the bulk melt (the bottom curve). As can be seen from comparative analysis of Figures 4 and 2, the behavior of energy curves in the case of slitlike pores is in qualitative agreement with the corresponding behavior for the cylindrical case. However, the influence of the slitlike pore width on the shift of temperature breakpoints and the distances between energy curves at low temperatures is essentially weaker than in the case of cylindrical capillaries. That is why the layered supports appear

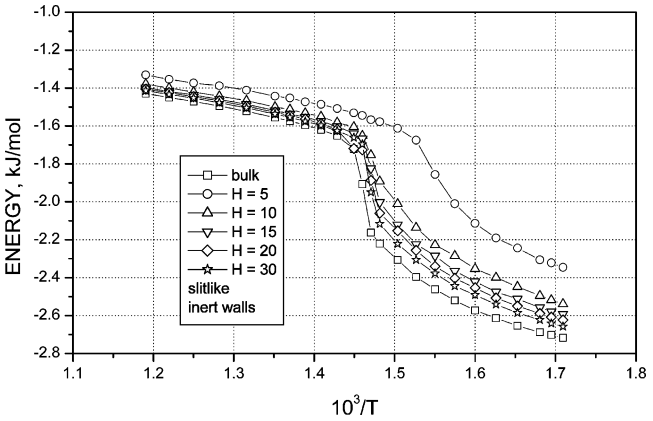

Figure 4. Calculated equilibrium potential energies per cell of melts confined by slitlike walls of different widths, *H*, vs inverse temperature: circles, $H = 5$; up triangles, $H = 10$; down triangles, $H = 15$; diamonds, $H = 20$; stars, $H = 30$; squares, $H =$ infinity (bulk melt).

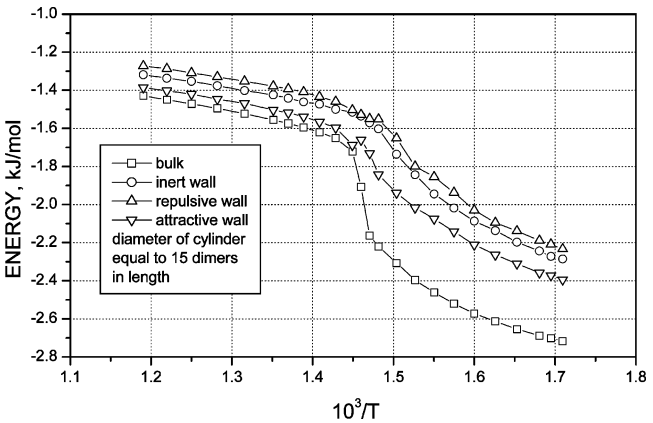

Figure 5. Comparison of the energetic contributions of repulsive, inert, and attractive cylindrical walls in the case of $d = 15$ dimers: up triangles, repulsive wall; circles, inert wall; down triangles, attractive wall; squares, bulk melt.

to be of little importance for the effective SO_2 oxidation at low temperatures.

Finally, Figure 5 shows the effect of repulsive, inert, and attractive walls of the cylindrical pore (15 dimers per diameter). The repulsive and inert walls yield almost the same values of an average potential energy per particle, although the repulsive curve lies a tiny bit higher than the inert one. The attractive cylindrical surface leads to slightly lower energy values at any

temperature. It seems that the minor differences between energy curves are mostly the consequence of the energetic contributions of pore walls.

Summary

The canonical Monte Carlo method was applied to study the temperature behavior of the lattice binary melt consisting of model $(V^{4+})_2$ and $(V^{5+})_2$ dimers confined by cylindrical and slitlike pore walls. It was found that (1) the smaller the pore size, the higher the retarding of the crystallization process, and (2) repulsive pore walls have only an insignificant influence on the crystallization process in agreement with inert ones, while attractive walls demonstrate a weak tendency to propagation of the crystallization process.

Besides, it was established that pore sizes of ~15 nm and smaller (for the case of nonlayered supports) provide the highest catalyst performance in SO_2 oxidation at low temperatures.

Acknowledgment. This work was in part supported by Russian Fund of Basic Research (Grant No. 99-03-32425).

References and Notes

(1) Kozyrev, S. V.; Bal'zhinimaev, B. S.; Boreskov, G. K.; Ivanov, A. A.; Mastikhin, V. M. *React. Kinet. Catal. Lett*. **1982**, *20*, 53.

(2) Ivanov, A. A.; Bal'zhinimaev, B. S. *React. Kinet. Catal. Lett.* **1987**, *35*, 413.

(3) Bal'zhinimaev, B. S.; Ivanov, A. A.; Lapina, O. B.; Mastikhin, V. M.; Zamaraev, K. I. *Faraday Discuss. Chem. Soc*. **1989**, *87*, 133 and references therein.

(4) Belyaeva, N. P.; Bal'zhinimaev, B. S.; Simonova, L. G.; Zaikovskii, V. I.; Ivanov, A. A.; Boreskov, G. K. *React. Kinet. Catal. Lett.* **1986**, *30*, 9.

(5) Oehlers, C.; Fehrmann, R.; Masters, S. G.; Eriksen, K. M.; Sheinin, D. E.; Bal'zhinimaev, B. S.; Elokhin, V. I. *Appl. Catal., A* **1996**, *147*, 127.

(6) Elokhin, V. I.; Myshlyavtsev, A. V.; Latkin, E. I.; Resnyansky, E. D.; Sheinin, D. E.; Bal'zhinimaev, B. S. *Kinet. Catal.* **1998**, *39*, 246.

(7) Latkin, E. I.; Sheinin, D. E.; Elokhin, V. I.; Bal'zhinimaev, B. S. *React. Kinet. Catal. Lett.* **1995**, *56*, 170.

(8) Bal'zhinimaev, B. S.; Belyaeva, N. P.; Reshetnikov, S. I. *Chem. Eng. Sci.* **1990**, *45*, 1939.

(9) Metropolis, N.; Rosenbluth, A. W.; Rosenbluth, M. N.; Teller, A. H.; Teller, E. *J. Chem. Phys.* **1953**, *21*, 1087.

(10) Metropolis, N.; Ulam, S. *J. Am. Stat. Assoc.* **1949**, *44*, 335.

(11) Eriksen, K. M.; Nielsen, K.; Fehrmann, R. *Inorg. Chem.* **1996**, *35*, 480.